Cancer Cell
Article

Calcification of Multipotent Prostate Tumor Endothelium

Andrew C. Dudley,[1] Zia A. Khan,[1] Shou-Ching Shih,[3] Soo-Young Kang,[1] Bernadette M.M. Zwaans,[1] Joyce Bischoff,[1] and Michael Klagsbrun[1,2,*]
[1]Vascular Biology Program
[2]Department of Surgery and Department of Pathology
Children's Hospital Boston and Harvard Medical School, Boston, MA 02115, USA
[3]Department of Pathology, Beth Israel Deaconess Medical Center and Harvard Medical School, Boston, MA 02215, USA
*Correspondence: michael.klagsbrun@childrens.harvard.edu
DOI 10.1016/j.ccr.2008.06.017

SUMMARY

Solid tumors require new blood vessels for growth and metastasis, yet the biology of tumor-specific endothelial cells is poorly understood. We have isolated tumor endothelial cells from mice that spontaneously develop prostate tumors. Clonal populations of tumor endothelial cells expressed hematopoietic and mesenchymal stem cell markers and differentiated to form cartilage- and bone-like tissues. Chondrogenic differentiation was accompanied by an upregulation of cartilage-specific *col2a1* and *sox9*, whereas osteocalcin and the metastasis marker osteopontin were upregulated during osteogenic differentiation. In human and mouse prostate tumors, ectopic vascular calcification was predominately luminal and colocalized with the endothelial marker CD31. Thus, prostate tumor endothelial cells are atypically multipotent and can undergo a mesenchymal-like transition.

INTRODUCTION

Tumor growth is angiogenesis dependent, and numerous studies have reported the eradication of tumors in mice by targeting the tumor vasculature (Folkman, 2007). Irrespective of these advances, very little is known about the biology of the endothelial cells (ECs) that line tumor blood vessels. An assumption of antiangiogenesis therapy is that tumor endothelial cells (TECs) are normal and derived from nearby, preexisting vessels. However, there are several key differences between normal and tumor endothelium. Tumor vessels are tortuous, leaky, and lack normal hierarchical organization (Baluk et al., 2005). Isolated TECs show increased drug resistance (Bussolati et al., 2003) and express distinct cell surface markers (Seaman et al., 2007; St Croix et al., 2000). Our laboratory has recently reported that TECs have aneuploid karyotypes (Hida et al., 2004) and express *ErbB1* (Amin et al., 2006). While the consequence of these abnormalities in TECs is at present unclear, it is possible that abnormal TECs could directly enable tumor growth, facilitate metastasis, and lead to acquired drug resistance to antiangiogenic therapies.

Most new blood vessels arise by co-option or sprouting of preexisting ECs. However, certain pathological conditions such as ischemia and cancer are known to depend on both EC sprouting and recruitment of circulating or bone marrow-derived endothelial progenitor cells (EPCs). For example, increased numbers of circulating EPCs can be detected following hindlimb ischemia (Takahashi et al., 1999), and bone marrow-derived EPCs are required for tumor growth in some tumor models (Lyden et al., 1999, 2001). On the other hand, studies using engraftment of GFP^+ bone marrow in tumor-bearing mice are equivocal. For example, the degree of bone marrow involvement may be time and/or tumor type dependent (Nolan et al., 2007). In some cases, direct incorporation of GFP^+ cells into tumor vessels has been observed (Davidoff et al., 2001; Duda et al., 2006; Santarelli et al., 2006; Yung et al., 2004). In other cases, GFP^+ cells were periendothelial, minimally incorporated into tumor vessels, or randomly scattered throughout the tumor (Larrivee et al., 2005; Machein et al., 2003; Rajantie et al., 2004; Udagawa et al., 2006). While these studies formally prove that bone marrow-derived progenitors are present in or around tumor blood vessels, one

SIGNIFICANCE

Endothelial cells line blood vessels that supply tumors with blood, nutrients, and oxygen during angiogenesis and act as a conduit for the removal of waste products. However, tumor blood vessels are poorly formed and dysfunctional. We have identified a multipotent, tumor-specific endothelial cell that undergoes calcification. Ectopic calcification of tumor endothelium may affect normal blood vessel function. For example, loss of the endothelial barrier in calcified tumor blood vessels could enable tumor cell intravasation into the blood stream or impair contractility and blood flow. Vascular calcification in tumors is easily discernible by standard histological techniques and may be useful as a diagnostic tool. Tumor blood vessel calcification adds to the growing list of abnormalities in tumor endothelium.

unanswered question has been whether or not TECs posses true stem- or progenitor-like properties such as multipotency and clonogenic ability.

Generally, stem cell fate is unidirectional and terminal. For example, hematopoietic stem cells (HSCs) give rise to all blood cell types of the lymphoid and myeloid lineages (Spangrude et al., 1988), whereas mesenchymal stem cells (MSCs) give rise to chondrocytes, osteoblasts, myoblasts, adipocytes, and neurons (Prockop, 1997). However, an unexpected finding in cancer stem cell research is that some tumor cells express genes associated with multiple cell types. One of the best known examples are melanoma tumor cells, which engage in vasculogenic mimicry by expressing endothelial-specific genes (VE-cadherin) and form fluid-transporting conduits (Hendrix et al., 2001). Thus, reprogramming of stem-like melanoma cells in the tumor microenvironment probably enables their adaptation and survival. It is plausible that other stromal progenitors in the tumor microenvironment could also acquire a multipotent, mutable phenotype due to reprogramming. Therefore, cellular plasticity may not be limited to putative cancer-forming stem cells but could also be common in tumor stromal cells such as ECs.

TRAMP (*tr*ansgenic *a*denocarcinoma of the *m*ouse *p*rostate) mice develop spontaneous prostate tumors beginning at puberty as androgens drive T antigen expression in prostatic secretory cells (Greenberg et al., 1995). An advantage of autochthonous tumor models such as TRAMP is that tumors are heterogeneous and subjected to selection pressure in the tumor microenvironment as they develop. Thus, tumors in TRAMP mice more closely mimic human cancers compared to xenografts. Angiogenesis in TRAMP mice has been well characterized in vivo, with vascular abnormalities beginning at the PIN (prostatic intraepithelial neoplasia) stage, which intensifies in poorly differentiated tumors (Ozawa et al., 2005). However, isolation and culture of ECs from TRAMP mice or any other autochthonous cancer model have not yet been described.

In the present study, we isolated TECs from spontaneously growing prostate tumors in TRAMP mice. Clonal populations of TECs could be differentiated to form bone- and cartilage-like tissues. These results suggest that TECs possess a stem/progenitor cell property that distinguishes them from ECs throughout the normal vasculature but undergo atypical transdifferentiation, possibly as a consequence of an osteogenic tumor microenvironment.

RESULTS

TECs Express Markers of Bona Fide Endothelium

Due to the small size of normal mouse prostate, it has been challenging to obtain enough tissue to isolate normal mouse prostate ECs. Thus, mouse dermal endothelial cells (MDECs) from C57BL/6 mice isolated in the same manner as TECs were used as a normal counterpart. In both TECs and MDECs, there was enriched expression of CD31, VEGFR-2, and vWF by semiquantitative RT-PCR (Figure 1A). However, CD146, a marker of mature or circulating ECs (Bertolini et al., 2006), was expressed in MDECs but not TECs. On the other hand, expression of the stem cell marker CD133 was between 2- and 3-fold higher in TECs compared to MDECs. Both ECs expressed the stem/hematopoietic marker c-Kit but were negative for the monocyte marker CD11b and the epithelial marker E-cadherin. The isolated TECs and MDECs had a cobblestone morphology and were uniformly positive for the endothelial markers CD31 and VE-cadherin but negative for the pericyte/mesenchymal marker αSMA by immunostaining (see Figure S1 available online). The expression of additional markers including CD31, VE-cadherin, VEGFR-2, PDGFR-β, SCA-1, CD34, and ID3 was evaluated by real-time PCR or western blotting and is shown in Figure S1.

TECs Express the Mesenchymal Marker CD90 and Form Blood Vessels When Engrafted into Nude Mice

Using flow cytometry, MDECs and TECs expressed comparable levels of CD31 and VEGFR-2 as single peaks on the histogram (Figure 1B). However, the EC/HSC marker CD34 was low to absent in TECs compared to MDECs, in good accord with the real-time PCR analysis (Figure S1). On the other hand, the MSC marker CD90 was lower in MDECs but was clearly expressed in TECs. The HSC/MSC marker SCA-1 was not expressed in TECs but was present in MDECs, consistent with SCA-1 expression in vascular endothelium (van de Rijn et al., 1989). Indeed, SCA-1$^-$/CD31$^+$ ECs were rare in TRAMP prostate tumors in vivo and constituted only 1% of the total EC population (Figure S2). In good agreement with the RT-PCR analysis, CD133 was about 2-fold higher in TECs relative to MDECs. Both MDECs and TECs were CD45$^-$, indicating absence of hematopoietic precursors. We found that the CD90$^+$/CD31$^+$ phenotype was consistent and stable in TECs from two separate isolations and was maintained after prolonged periods in culture (Figures 1C and 1D). To demonstrate EC functionality, GFP-expressing TECs were prepared by pMX-GFP retroviral infection as described previously (Kitamura et al., 1995). MDECs and TECs formed tube-like structures when cultured within a Matrigel plug in vitro and were positioned at the luminal surface of erythrocyte-filled blood vessels when injected in vivo (Figures 1E–1G). Taken together, MDECs and TECs expressed the expected mature EC markers and functioned as bona fide endothelium, but the expression of HSC and MSC markers in TECs was atypical.

TECs Form Mesenchymal-like Foci in Culture and Demonstrate Alkaline Phosphatase Activity When Cultured in Osteogenic Medium

Preliminary experiments indicated that MDECs and TECs were not functional hematopoietic progenitors based on the absence of colony-forming units in methylcellulose (data not shown). TECs had an MSC-like profile (CD90$^+$/CD34$^-$) and formed foci in culture, reminiscent of MSCs (Figure 2A). However, the morphology of TEC foci was distinct from that of MSC foci. TECs were cuboidal and did not overlap at their margins, in contrast to spindle-shaped, overlapping MSCs (Figure 2B). We next tested whether TECs could differentiate to form mesenchymal lineages such as osteocytes or adipocytes using selective media. In adipogenic medium, about 50% of bone marrow-derived mesenchymal stem cells (BM-MSCs) differentiated to form lipid-storing adipocytes based on oil red O staining (Figures 2C and 2D). On the other hand, neither TECs nor MDECs showed any evidence of oil red O staining when cultured under the same conditions. In osteogenic medium, about 95% of BM-MSCs showed areas of alkaline phosphatase (ALP) activity and about 10% of TECs were ALP positive, indicating osteogenic differentiation. MDECs were completely ALP negative. In TECs, ALP activity colocalized

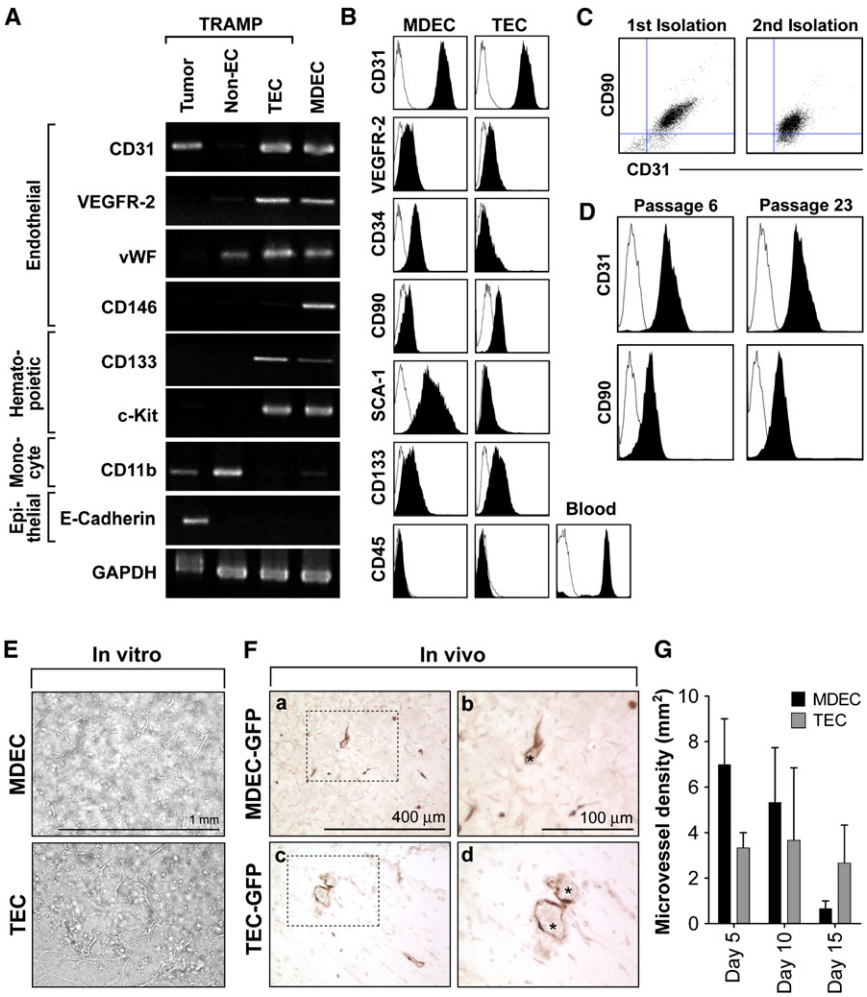

Figure 1. Tumor Endothelial Cells Express Markers of and Function as Bona Fide Endothelium

(A) Isolated tumor endothelial cells (TECs) and mouse dermal endothelial cells (MDECs) (both passage 6) were analyzed for marker expression by RT-PCR. The unfractionated tumor and the $CD31^-$ non-EC fractions from the purification step were also included on the gel.

(B) Fluorescence-activated cell sorting (FACS) demonstrating uniform staining for the selected markers in MDECs and TECs.

(C) FACS analysis of $CD31^+/CD90^+$ TECs from two separate isolations. Three to four tumors were pooled in each example, and ECs were isolated and expanded in culture as described.

(D) The $CD31^+/CD90^+$ phenotype was stable and was observable after prolonged culture.

(E) Both MDECs and TECs formed tube-like structures in a three-dimensional Matrigel culture system in vitro.

(Fa–Fd) GFP-tagged MDECs and TECs formed functional blood vessels when injected in vivo. Matrigel plugs from day 10 were stained with anti-GFP antibodies. The staining shows the luminal position of the labeled ECs (dark brown staining). The boxed regions are shown at higher magnification at right. Visible erythrocytes within the vessels are marked with an asterisk (*).

(G) Microvessel density over time (n = 3 mice per group). Error bars represent ± SEM.

with the endothelial marker CD31 in these areas of differentiation (data not shown). These results suggested that TECs might undergo a mesenchymal differentiation, prompting us to further investigate this possibility.

TECs Undergo Mineralization after Prolonged Culture in Osteogenic Medium

The von Kossa reaction detects calcification following the precipitation of silver phosphate at sites of high concentrations of inorganic phosphate (particularly calcium phosphate formed by osteoblasts). No von Kossa staining was present in MDECs or TECs after 2 weeks in osteogenic medium (Figure 3A). However, after 3 weeks in differentiation medium, von Kossa staining was detected in TECs but not MDECs. In good accord with these results, the late markers of osteogenic differentiation osteopontin (*ssp1*) and osteocalcin (*bglap*) were upregulated between 3- and 6-fold in TECs only after 3 weeks in osteogenic medium (Figures 3B and 3C). These results were consistent with TEC osteogenic differentiation in vitro.

Chondrogenic Differentiation of TECs

We further tested for TEC multipotency by incubating cells in chondrogenic medium containing TGF-β for up to 2 weeks (Pittenger et al., 1999). TECs and BM-MSCs formed visible pellets after approximately 3–4 days in culture, while MDECs never formed visible cell pellets under these conditions. Chondrogenic differentiation was confirmed by positive staining for Alcian blue and col2a1 in the sectioned pellets (Figure 4A). Normal mouse leg served as a control where articular cartilage around the knee stained specifically for Alcian blue and col2a1. Exchanging TGF-β1 for TGF-β3 resulted in no visible pellet in TECs. Accordingly, TGF-β3 resulted in marked upregulation of mRNAs for chondrocyte-specific *col2a1* (11-fold) and the master chondrogenic transcription factor, *sox9* (12-fold) (Figures 4B and 4C).

TECs Can Be Grown as Single-Cell Clones

To rule out the possibility of contamination with mesenchymal precursors, we prepared single-cell clones of TECs. Limiting dilution assays revealed single cells in individual wells that only occasionally (<0.5%) formed proliferating colonies. A single, highly proliferative clone of TECs obtained by limiting dilution (clone G9) formed mesenchymal-like foci and flattened, cuboidal-shaped cells when confluent (Figure 5A). We were unable to obtain single-cell clones of MDECs by limiting dilution; however, clones of MDECs could be readily obtained using cloning rings on colonies of sparsely plated cells. In TEC clone G9, CD31 double staining showed coexpression with the MSC markers CD90, CD44, and CD105, but not SCA-1 (Figure 5B). In contrast, an isolated colony of MDECs were double positive for CD31, CD44,

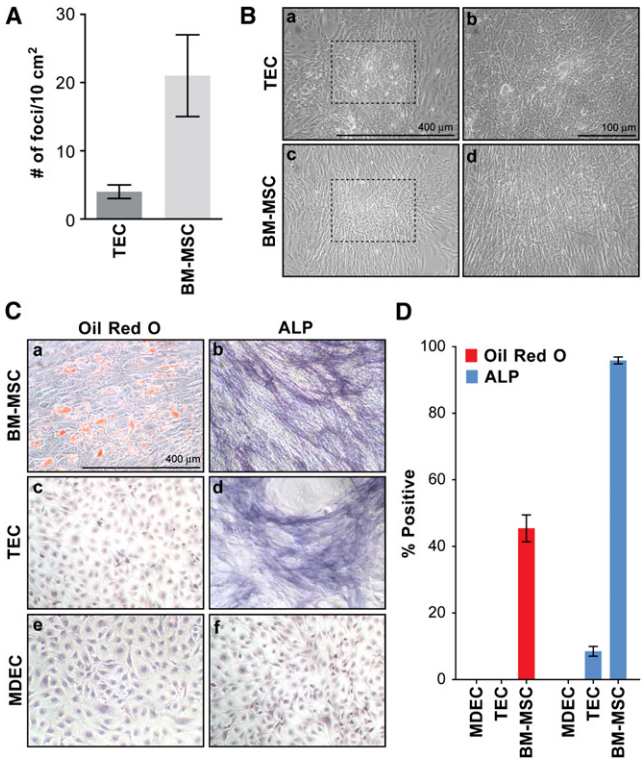

Figure 2. TECs Form Mesenchymal-like Foci In Vitro and Demonstrate Alkaline Phosphatase Activity When Cultured in Osteogenic Medium

(A) Foci in TECs and bone marrow-derived mesenchymal stem cells (BM-MSCs) were counted and averaged from two 10 cm^2 culture dishes.

(Ba–Bd) The morphology of TEC foci was cuboidal (Ba and Bb) with no overlap between adjacent cells, while BM-MSCs were spindle-shaped with overlapping borders (Bc and Bd). The boxed regions at left are shown in higher magnification at right.

(Ca–Cf) BM-MSCs underwent adipogenic differentiation (Ca) and upregulated alkaline phosphatase (ALP) activity (Cb) after culture in adipogenic or osteogenic medium, respectively. TECs did not undergo adipogenic differentiation (Cc) but did show an upregulation of ALP activity in osteogenic medium (Cd). MDECs did not differentiate under any test conditions (Ce and Cf). In (Cc), (Ce), and (Cf), nuclei were counterstained with hematoxylin.

(D) The percentages of cells positive for oil red O and ALP from ten fields were quantified and plotted on the graph.

Error bars in (A) and (D) represent ± SEM.

CD105, and SCA-1 but low to absent for CD90. BM-MSCs were positive for all MSC markers but did not express CD31 as expected.

Single-Cell Clones of TECs Undergo Osteogenic and Chondrogenic Differentiation

Similar to the parental TEC population, TEC G9 underwent mineralization when cultured in osteogenic medium, indicated by blackish-brown von Kossa staining (Figure 6A). TEC G9 also formed a visible pellet in chondrogenic differentiation medium that, when sectioned, stained positive for Alcian blue. However, TEC G9 failed to undergo adipogenic differentiation, in contrast to BM-MSCs, where intracellular lipids were stained with oil red O. As expected, RT-PCR analysis showed that MDECs failed to upregulate lineage-specific markers in all differentiation media (Figure 6B). Consistent with TECs' failure to undergo adipogenic differentiation, PPARγ2 was almost undetectable in TEC G9 after culture in adipogenic medium, in contrast to BM-MSCs. On the other hand, both TEC G9 and BM-MSCs upregulated *col2a1* and osteopontin mRNAs in chondrogenic and osteogenic differentiation media, respectively. CD31 was coexpressed in TECs and MDECs under all conditions but was qualitatively diminished in TECs cultured in differentiation media. An additional clone (TEC A2) obtained by limiting dilution had a $CD90^+/CD31^+$ phenotype (data not shown) and could be induced to express *col2a1* and osteopontin, but not the adipogenic marker PPARγ2 (Figure 6C). Taken together, these results suggest that TECs are clonogenic and can undergo atypical multilineage differentiation but do not undergo adipogenic differentiation characteristic of bona fide BM-MSCs.

In Vivo Calcification of Prostate Tumor Cells and Vascular Cells

To determine whether calcification is a feature of vascular cells in clinical cancers, we used human prostate tissue arrays with tumors of various grades. Low levels of von Kossa staining were detected in 1 of 8 matched control prostate tissue specimens, but 22 of 36 prostate tumor specimens (61%) showed varying degrees of von Kossa staining (Figure 7A; Table 1). Eleven percent of these specimens were characterized by densely black, localized granules, characteristic for von Kossa staining, whereas between 22% and 28% showed less robust staining or individually stained cells throughout the tumor. Some von Kossa staining was near necrotic regions in these tumors. While no von Kossa staining was detected in blood vessels from normal prostate tissues, 11% of tumor specimens showed vascular staining that was localized to the lumen or within the blood vessel wall (Figure 7B; Figure S3). von Kossa staining was often localized with the endothelial marker CD31 and the pericyte marker αSMA, confirming the vascular-specific pattern (Figure 7C). Of a total of 368 $CD31^+$ tumor blood vessels counted, 13 vessels (~4%) were also stained with von Kossa, confirming the endothelial sites of calcification. All of these data are summarized in Table 1. Finally, in TRAMP mice, the chondrocytic marker col2a1 and von Kossa staining were also detected in prostate tumors and tumor blood vessels (Figure S4). Thus, TECs in clinical prostate cancers and TRAMP mice are characterized by an atypical transdifferentiation into mesenchymal lineages.

DISCUSSION

This study describes the isolation and characterization of TECs from spontaneously growing prostate tumors in TRAMP mice. Similar to normal ECs, TECs had a cobblestone or cuboidal morphology and expressed markers such as CD31, VE-cadherin, and VEGFR-2. In contrast, TECs did not express SCA-1, CD34, or CD146, markers common to most vascular ECs, but did express CD90. CD90, also known as Thy-1, is a marker that is not typically found in quiescent endothelium (Lee et al., 1998) but is instead expressed by mesenchymal progenitors. Interestingly, Thy-1 was also found to be highly expressed in human tumor-derived ECs in the seminal study by St Croix et al. (2000). TECs were also clonogenic and differentiated to form bone- and cartilage-like tissues when cultured in selective

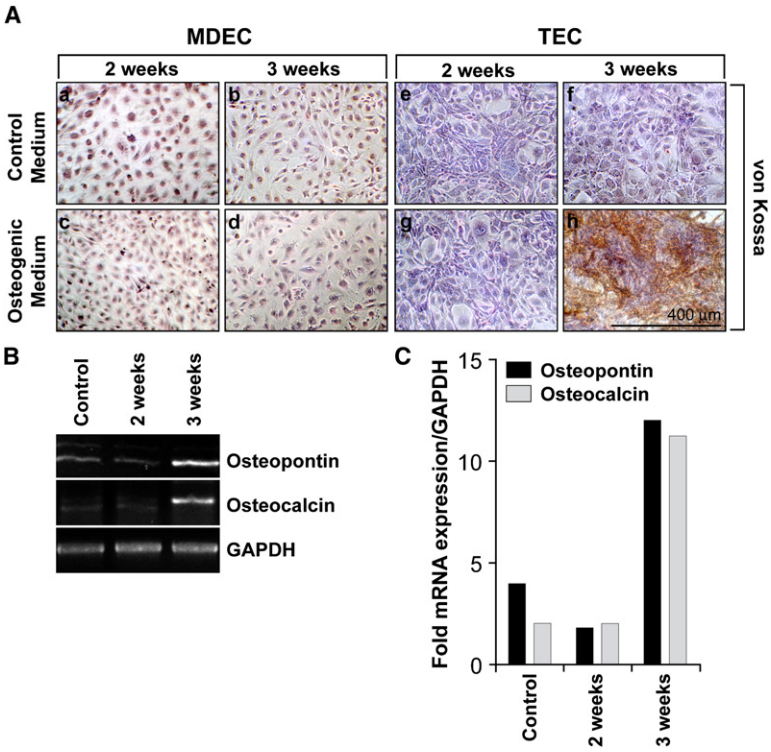

Figure 3. TECs Undergo Mineralization after Prolonged Culture in Osteogenic Medium

(Aa–Ah) MDECs were negative for von Kossa staining in control and osteogenic medium after a 2 week (Aa and Ac) or 3 week incubation (Ab and Ad). TECs were also von Kossa negative after the 2 week incubation (Ae and Ag), but intense von Kossa staining, indicating calcification, was present in TECs after 3 weeks (Af and Ah). Nuclei were counterstained with hematoxylin.

(B and C) After 3 weeks in osteogenic medium, the late markers of osteogenic differentiation osteopontin and osteocalcin were upregulated ~3-fold and ~5-fold, respectively, in TECs.

media. TECs were not tumor cells masquerading as ECs, nor were they contaminated with tumor cells, as indicated by absence of T antigen expression in vivo and in vitro (Figure S5). However, absence of T antigen expression in TECs does not preclude the possibility that tumor epithelial cell transformation in the prostate does not result in epigenetic alterations in the associated stromal cells, as documented in human breast carcinoma (Hu et al., 2005). Taken together, several lines of evidence suggest that TECs can undergo transdifferentiation into mesenchymal lineages: (1) single-cell clones of TECs underwent differentiation into bone and cartilage; (2) potential contamination with bona fide MSCs was precluded because TECs could only differentiate into bone and cartilage but not adipocytes; (3) TECs expressed EC markers such as CD31 and VE-cadherin, which are absent in MSCs; and (4) CD31 protein and bone-related differentiation markers (ALP) were present in the same cells.

What is the origin of TECs? The majority of ECs in tumor blood vessels probably arise by sprouting from nearby, preexisting ECs. However, the turnover of ECs in vivo is extremely slow (approximately one cell division every 1000 days) but increases dramatically during active angiogenesis. Hierarchies of resident EPCs with different clonogenic and proliferative abilities reside throughout the vasculature, even into adult life (Ingram et al., 2004, 2005). Resident EPCs may form the immediate angiogenic response to tissue injury by circumventing systemic bone marrow involvement (O'Neill et al., 2005). Similarly, tissue-resident progenitors may form the immediate response to tumor angiogenesis. For example, multipotent $CD34^-$ tissue-resident progenitors with potential to differentiate into mesodermal and mesenchymal lineages (Jiang et al., 2002; Reyes et al., 2001) and incorporate into tumor blood vessels have recently been described (Bussolati et al., 2005). However, the identification and relative contribution of tissue-resident progenitors to tumor vasculature has been difficult to address, probably due to the rarity of these cells in adult tissue.

On the other hand, bone marrow-derived and circulating EPCs play a definitive role in tumor growth in some tumor models, where they may mediate a postulated metastatic switch (Gao et al., 2008). Furthermore, the $ID1^{+/-}$ $ID3^{-/-}$ knockout mouse, which has delayed tumor growth and poorly vascularized tumors, fails to incorporate bone marrow-derived progenitors into tumor blood vessels (Lyden et al., 1999, 2001). While our isolated TECs strikingly overexpressed ID3 in culture, they did not express the HSC markers SCA-1 or CD34. Together, this was an unusual expression profile for an EC, but it was not entirely indicative of a bone marrow-derived progenitor. Instead, the complete absence of SCA-1 expression in TECs and the rarity of $CD31^+/SCA\text{-}1^-$ ECs in prostate tumors in vivo could indicate a possible tissue-resident, rather than a bone marrow-derived, origin.

While it appears that TECs are progenitor- or stem-like cells, normal ECs do not usually undergo a mesenchymal transition—two exceptions are the rare cardiac valve ECs in developing cardiac cushions (Paruchuri et al., 2006) and embryonic ECs in the dorsal aorta (DeRuiter et al., 1997). It is interesting that a common mesodermal ancestor for ECs and pericytes has been postulated (Yamashita et al., 2000) given that pericytes are not terminally differentiated cells and can differentiate into fibroblasts, osteoblasts, chondrocytes, and adipocytes (Doherty et al., 1998; Farrington-Rock et al., 2004). Furthermore, MSCs themselves may give rise to endothelium under pathobiological conditions (Wang et al., 2005). One possibility is that some TECs arise from mesenchymal progenitors and undergo a mesenchymal-like differentiation due to factors in the tumor microenvironment. By culturing isolated TECs in defined differentiation media, we were able to recapitulate this phenomenon in vitro. Thus, tumor stromal cells, like cancer stem cells, may be capable of multipotent differentiation into atypical lineages (Hendrix et al., 2007; Topczewska et al., 2006).

Ectopic bone and cartilage, osteoclast-like cells, and calcifying vascular cells have been described in diseased blood vessel wall (Tintut et al., 2003; Watson et al., 1994). For example, vascular calcifications are common in the medial layer around atherosclerotic plaques. Angiogenesis is abundant in these areas

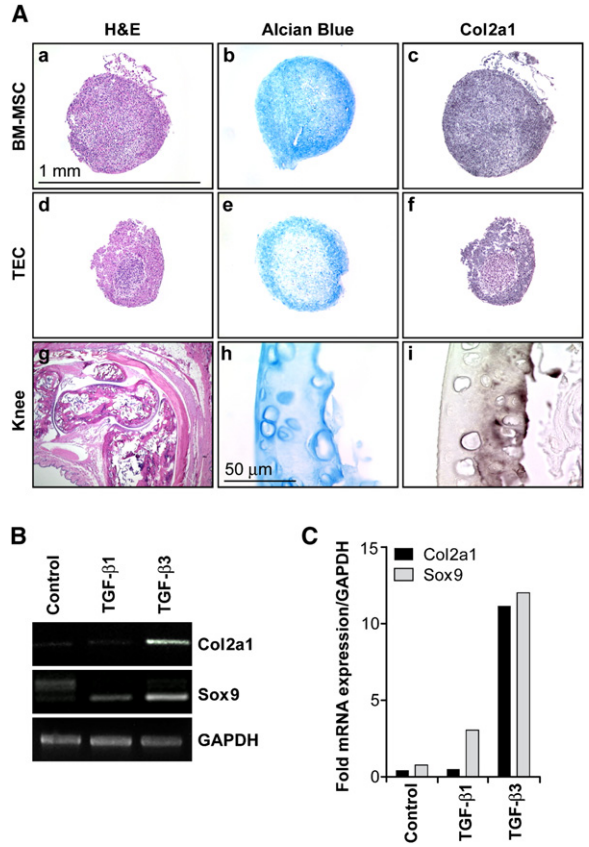

Figure 4. Chondrogenic Differentiation of TECs

(Aa–Ai) BM-MSCs and TECs formed a visible pellet within 3–4 days that was maintained for the 2 week experiment. Formalin-fixed, paraffin-embedded pellets were sectioned and stained with hematoxylin and eosin (H&E; Aa and Ad), Alcian blue (Ab and Ae), or col2a1 antibodies (Ac and Af). An H&E-stained section of mouse leg is also shown (Ag). Articular cartilage around the knee stained specifically with Alcian blue (Ah) and col2a1 (Ai). The 1 mm scale bar applies to panels (Aa)–(Ag); the 50 μM scale bar applies to panels (Ah) and (Ai). (B and C) The markers of chondrogenic differentiation *col2a1* and *sox9* were upregulated ~12-fold in TECs in the presence of TGF-β3. No pellet was formed in TECs when TGF-β1 was substituted.

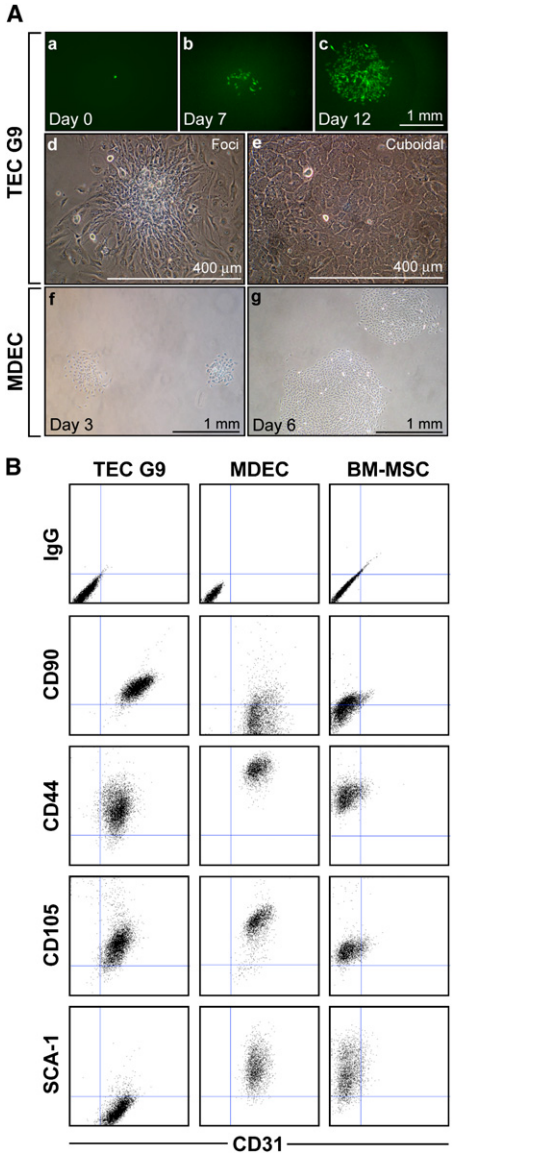

Figure 5. TECs Can Be Grown as Single-Cell Clones

(Aa–Ag) TECs infected with retroviral GFP were plated as single cells in 96-well plates. While most single cells never proliferated, occasional colonies could be obtained from single cells (Aa) that proliferated into clonal populations 7 days (Ab) and 12 days (Ac) after seeding. TEC clone G9 obtained by limiting dilution formed foci (Ad) and highly proliferative, cuboidal-shaped cells (Ae). Single-cell clones could not be obtained in MDECs by limiting dilution, but sparsely plated MDECs readily formed colonies that could be selected using cloning rings. MDECs are shown 3 days (Af) and 6 days (Ag) after initial plating, but before selection using cloning rings.

(B) Flow cytometry was carried out on live cells using the indicated antibodies. Consistent with the parental TECs, clone G9 coexpressed CD90 and CD31. The additional mesenchymal markers CD44 and CD105 were also present while SCA-1 was absent in TECs. A colony of MDECs selected using cloning rings expressed CD31 in addition to CD44, CD105, and SCA-1, but CD90 was low to absent. BM-MSCs expressed all markers with the exception of CD31.

of lesional calcification, with newly formed vessels proliferating around the calcified deposits (Johnson et al., 2006). The interactions between bone morphogenetic proteins, VEGF, pericytes, and resident osteoprogenitor cells are thought to account for cardiac valve and arterial calcification (Collett and Canfield, 2005). Notably, in most vascular diseases, calcification is typically observed in the extracellular matrix surrounding smooth muscle cells in the arterial wall, whereas in human prostate tumors, we observed calcification mainly at the luminal side of capillaries. Therefore, at least in prostate tumors, TECs appear to undergo a mesenchymal-like transition to form bone-like tissues. Interestingly, TECs cultured in osteogenic medium in vitro transitioned from cobblestone- into spindle-shaped cells. It is possible that loss of cell-to-cell contact in calcified tumor blood vessels in vivo could impair blood flow or enable tumor cell intravasation into the bloodstream, facilitating metastasis.

An osteogenic tumor microenvironment in prostate cancer has been hypothesized to facilitate metastasis to bone (Chung, 2003; Edlund et al., 2004). For example, the expression of bone-specific proteins in prostate tumor cells may enable their survival once they reach the bone microenvironment (Koeneman

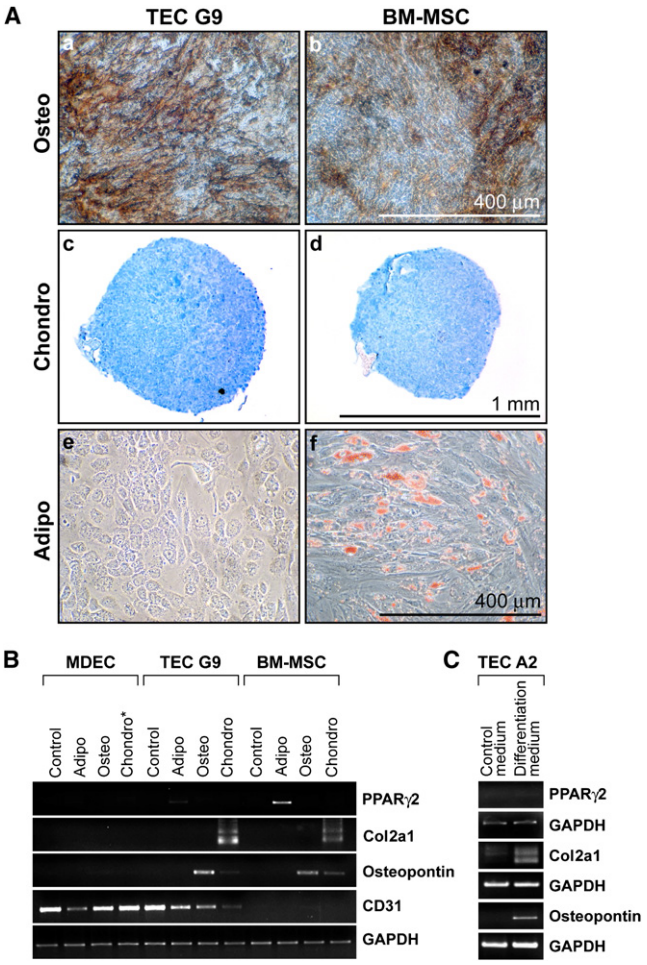

Figure 6. Single-Cell Clones of TECs Undergo Osteogenic and Chondrogenic Differentiation

(Aa–Af) After 3 weeks in osteogenic medium, TEC clone G9 was formalin-fixed and stained with von Kossa solution. Brownish/black staining in G9 (Aa) and BM-MSCs (Ab) was evident, indicating calcification. Chondrogenic differentiation was also observed in clone G9 (Ac) and BM-MSCs (Ad), indicated by a visible pellet after 2 weeks in chondrogenic medium that stained with Alcian blue. In adipogenic medium, no oil red O-positive cells were observed in clone G9 (Ae), in contrast to BM-MSCs (Af).

(B) Semiquantitative RT-PCR analysis for differentiation markers in each cell type cultured in the indicated differentiation medium. The asterisk (*) indicates that 5% serum was included in the chondrogenic medium because MDECs did not survive in the serum-free conditions.

(C) *col2a1* and osteopontin, but not PPARγ2, were inducible in an additional TEC clone (A2) cultured in differentiation medium.

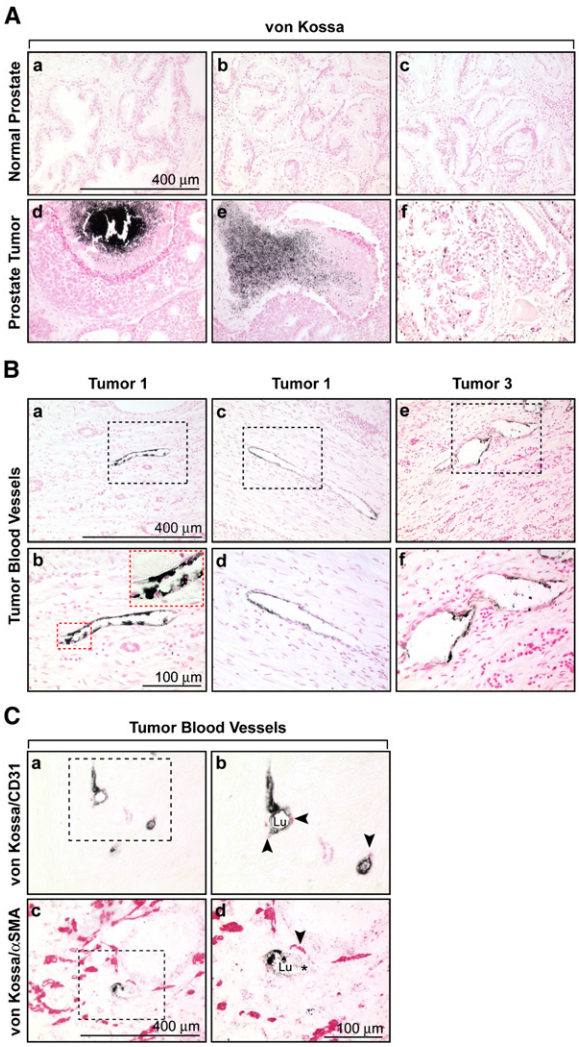

Figure 7. In Vivo Calcification of Prostate Tumor Cells and Vascular Cells

(Aa–Af) Representative images of von Kossa staining in normal prostate (Aa–Ac) and prostate tumors (Ad–Af). Calcification in tumors was often associated with highly necrotic regions.

(Ba–Bf) von Kossa staining in tumor blood vessels from three different tumors showing the luminal localization (Aa, Ac, and Ae). Boxed regions in the upper row are shown in higher magnification in the lower row (Ab, Ad, and Af). The inset in (Ab) shows a higher magnification of the boxed region. Nuclei in (A) and (B) were counterstained with nuclear fast red.

(Ca–Cd) Colocalization of the endothelial marker CD31 (Ca and Cb) and the pericyte marker αSMA (Cc and Cd) with von Kossa staining in tumor blood vessels. The boxed regions at left are shown in higher magnification at right. CD31 and αSMA were detected using an alkaline phosphatase-conjugated secondary antibody and appear red in the figure. No counterstain was used. Lu = lumen; the asterisk (*) marks a visible erythrocyte within the vessel lumen in (Cd).

et al., 1999). Here, we describe the expression of typically bone-restricted markers such as ALP, osteocalcin, and osteopontin in TECs. Osteopontin is widely used as a biomarker for advanced disease and is a known mediator of bone metastasis (Kang et al., 2003; Nemoto et al., 2001; Wai and Kuo, 2008). Osteopontin contains an RGD motif that mediates cell-to-cell interactions through integrins facilitating anchorage-independent growth and invasion (Allan et al., 2006). Thus, osteopontin expression in TECs could be chemotactic for tumor cells, enabling their interaction with blood vessels and allowing for intravasation. Similarly, serum osteocalcin is elevated in patients with bone-metastatic prostate cancer, where it is primarily a biomarker of bone deposition (Hegele et al., 2007). *sox9*, a transcriptional regulator of *col2a1* during chondrogenesis, was inducible in TECs and is expressed in prostate cancer cells, where it regulates androgen receptor expression (Wang et al., 2007). The chondrocytic marker col2a1, which has not been described as a marker

Table 1. Quantification of von Kossa Staining in Normal Prostate and Prostate Tumors

	Number of Specimens with von Kossa Staining	Number of Specimens with von Kossa Staining in Blood Vessels	Total Number of CD31$^+$/von Kossa$^+$ Blood Vessels
Normal prostate	1/8[a]	0/8	ND
Prostate tumor (total)	22 (61 %)	4/36 (11 %)	13/368 (~4 %)
Low	10 (28 %)		
Medium	8 (22 %)		
High	4 (11 %)		

Prostate tumor cores of various grades (n = 36) were matched with adjacent normal prostate tissue (n = 8). ND = none detected.
[a] One normal prostate had low levels of diffuse von Kossa staining, but not in blood vessels.

of tumor blood vessels, was also present in prostate tumor specimens and tumor endothelium, but not in normal prostate. Thus, factors normally expressed in bone, cartilage, or prostate tumor cells are inducible in TECs but not normal ECs. One possibility is that osteogenic factors in the tumor microenvironment may induce the osteogenic and chondrogenic differentiation of tissue-resident or bone marrow-derived progenitors in the tumor stroma.

In conclusion, it has long been assumed that TECs were identical to normal ECs. For example, human umbilical vein endothelial cells (HUVECs) are a common surrogate for studying the efficacy of antiangiogenic drugs in vitro. However, morphological (McDonald and Choyke, 2003), pathophysiological (Hagendoorn et al., 2006), cytogenetic (Hida et al., 2004; Streubel et al., 2004), epigenetic (Grover et al., 2006), gene expression (St Croix et al., 2000), and, here, atypical multipotent plasticity have all been demonstrated in TECs. It will now be important to determine whether the mutable properties of prostate TECs relate to abnormalities in tumor blood vessels, whether vascular calcification might enable tumor cell metastasis or impair blood flow, and whether vascular calcification in tumors could be used as a diagnostic tool.

EXPERIMENTAL PROCEDURES

Cells and Media

TECs and MDECs were cultured in low-glucose DMEM containing antibiotic/antimycotic, 10% FBS, 10% Nu-Serum IV (BD PharMingen), 3 ng/ml bFGF, 50 ng/ml VEGF (both bFGF and VEGF were kind gifts from the NCI Biological Resources Branch Preclinical Repository), and 100 mg/l porcine heparin (Sigma-Aldrich). BM-MSCs were cultured in the same medium, but with 20% FBS added. All cells were used between 12 and 15 passages.

Mice

TRAMP mice (C57BL/6) were housed in compliance with Children's Hospital Boston guidelines, and all animal-related protocols were approved by the Institutional Animal Care and Use Committee. Mice were genotyped at weaning (Transnetyx).

TEC Isolation

Large prostate tumors typically arose by 30–40 weeks of age in TRAMP mice. Tumors were minced with fine scissors into pieces < 1 mm in size. Minced tumors were then transferred to HBSS containing 1 mg/ml collagenase type I (Worthington Biochemical Corporation) and 100 μg/ml DNase (Worthington) and placed in a 37°C water bath. The sample was alternately vortexed and disrupted by trituration every 10 min over a 30–45 min period until the mixture could be freely pipetted. Next, tumor digests were filtered with a 100 μm cell strainer and centrifuged at 1200 rpm for 15 min. The cell pellet was then resuspended in 1× PharmLyse B (BD PharMingen), and left at room temperature for 10 min. After the 10 min incubation, the sample was centrifuged at 1200 rpm for 5 min, and the cell pellet was resuspended in 10 ml of MACS buffer (degassed phosphate-buffered saline [PBS] containing 2 mM EDTA and 0.5% BSA) and filtered again through a 70 μm cell strainer. Cells were centrifuged as before, and approximately 250 μl of packed cells was resuspended in 500 μl of MACS buffer. Ten micrograms of rat anti-mouse CD31 antibody (BD PharMingen) was added to the resuspended cells, which were incubated at room temperature for 10 min. After the 10 min incubation, cells were centrifuged as above and washed twice with MACS buffer. The cells were resuspended in 320 μl of MACS buffer, and 80 μl of goat anti-rat magnetic beads was then added (Miltenyi Biotec). The mixture was left at room temperature for another 10 min and then filtered through a 100 μm cell strainer before being passed over a magnetic column (Miltenyi Biotec). After washing the column with 8–10 ml of MACS buffer, the bound cells were eluted. The eluted cells were centrifuged and washed three times with culture medium before plating into a T-75 flask coated with 10 μg/ml of human fibronectin (Biomedical Technologies). After 4–6 weeks, cells were washed with PBS and detached using 3 ml of Accutase (Innovative Cell Technologies). Cells were centrifuged, washed once with MACS buffer, and resuspended in 200 μl of MACS buffer containing 10 μg of rat anti-mouse ICAM-2 antibodies (BD PharMingen). The purification procedure was repeated as above. The purified ECs eluted from the magnetic column were washed twice with culture medium and then seeded into a single well of a six-well or 24-well plate. The use of cloning rings was often necessary as a final method for obtaining pure endothelial cell cultures.

Differentiation

For adipogenic differentiation, cells were seeded at a density of 50,000 cells/well in 12-well plates. The next day, the medium was removed and replaced with DMEM containing 1% antibiotic/antimycotic, 10% FBS, 5 μg/ml insulin, 1 μM dexamethasone, 0.5 μM isobutylmethylxanthine, and 60 μM indomethacin (all reagents purchased from Sigma-Aldrich). After 2 weeks, cells were washed, fixed in formalin, and stained with oil red O to detect lipid. For osteogenic differentiation, cells were plated into two-well chamber slides in medium containing DMEM, 10% FBS, 1% antibiotic/antimycotic, 1 μM dexamethasone, 10 mM β-glycerophosphate, and 100 μM ascorbic acid 2-phosphate. After 1–3 weeks, cells were washed, fixed in formalin, and stained for ALP or von Kossa solution (Diagnostic BioSystems). For chondrogenic differentiation, cells were detached with Accutase, washed, adjusted to 1×10^6 cells/ml, and centrifuged. The medium was carefully aspirated and replaced with high-glucose DMEM containing 1% antibiotic/antimycotic, 10 μl/ml insulin-transferrin-selenium, 1 μM dexamethasone, 20 ng/ml TGF-β1 or TGF-β3 (R&D Systems), and 100 μM ascorbic acid 2-phosphate. In all experiments, control medium was DMEM containing 10% FBS with 1% antibiotic/antimycotic.

Fluorescence-Activated Cell Sorting

Cell were detached with Accutase, washed, and resuspended in PBS/0.1% BSA containing the indicated conjugated antibodies (all purchased from BD PharMingen, with the exception of CD90, CD105, and CD44 antibodies, which were purchased from eBioscience). After two washes, cells were analyzed using a BD FACSCalibur System (BD Biosciences).

RT-PCR

Total cellular RNA was extracted using an RNeasy kit according to the manufacturer's directions (QIAGEN). Five micrograms of RNA was subjected to

reverse transcription by standard methods. Two microliters of cDNA was then used in a 50 μl PCR reaction containing a 1 μM concentration of each primer, 1 μl of dNTPs (10 mM stock), 5 μl of 10× PCR buffer with $MgCl_2$ (Invitrogen), and 0.4 μl of *Taq* DNA polymerase (Roche).

Immunofluorescence

Cells were seeded at a density of 10,000 cells per well in fibronectin coated eight-well chamber slides. Confluent cells were washed twice with PBS and then fixed with ice-cold 100% methanol at −20°C for 20 min. The fixed cells were rinsed briefly with PBS and then blocked for 1 hr at room temperature with PBS containing 5% BSA. After blocking, antibodies were added overnight at 4°C in a humidified chamber. The next day, cells were rinsed with PBS and then blocked again for 30 min at room temperature. Secondary antibodies were added, and the cells were incubated for an additional 1 hr at room temperature protected from light. Finally, cells were washed with PBS and then mounted using Gel Mount (Biomeda) containing 0.4 μg/ml 4′,6-diamidino-2-phenylindole (DAPI).

Matrigel Plug Assay

Two million TECs and MDECs were washed and resuspended in 100 μl of phenol red-free Matrigel. For the in vitro tube-forming assay, 50 μl of this suspension was pipetted into single wells of a 24-well plate and then placed at 37°C for 20 min. Each well was then filled with 1 ml of EC growth media. For the in vivo experiment, 2×10^6 TECs or MDECs were resuspended in Matrigel and injected into the lateral flank of 8-week-old nu/nu mice. Implants were removed on the indicated days and fixed in formalin overnight.

Tissue Microarrays

Commercially available human prostate adenocarcinoma tissue arrays were purchased from Biomax US. The array had 48 cores in duplicate with tissue-matched controls. Under the guidelines of the Clinical Investigation Policy and Procedure Manual at Children's Hospital Boston, commercially available specimens that cannot be linked to subjects are exempt from IRB review.

SUPPLEMENTAL DATA

The Supplemental Data include five figures and can be found with this article online at http://www.cancercell.org/cgi/content/full/14/3/201/DC1/.

ACKNOWLEDGMENTS

This work was supported by NIH grants CA37392 and CA45548. A.C.D. wishes to thank Leonora DeBella and the American Cancer Society for supporting his research with a postdoctoral fellowship. We thank K. Johnson for excellent assistance with figures, P. Hauschka for critically reviewing the manuscript, and J. Melero-Martin for assistance with immunohistochemistry and EPCs. We dedicate this work in memory of Dr. Judah Folkman.

Received: October 17, 2007
Revised: April 22, 2008
Accepted: June 27, 2008
Published: September 8, 2008

REFERENCES

Allan, A.L., George, R., Vantyghem, S.A., Lee, M.W., Hodgson, N.C., Engel, C.J., Holliday, R.L., Girvan, D.P., Scott, L.A., Postenka, C.O., et al. (2006). Role of the integrin-binding protein osteopontin in lymphatic metastasis of breast cancer. Am. J. Pathol. *169*, 233–246.

Amin, D.N., Hida, K., Bielenberg, D.R., and Klagsbrun, M. (2006). Tumor endothelial cells express epidermal growth factor receptor (EGFR) but not ErbB3 and are responsive to EGF and to EGFR kinase inhibitors. Cancer Res. *66*, 2173–2180.

Baluk, P., Hashizume, H., and McDonald, D.M. (2005). Cellular abnormalities of blood vessels as targets in cancer. Curr. Opin. Genet. Dev. *15*, 102–111.

Bertolini, F., Shaked, Y., Mancuso, P., and Kerbel, R.S. (2006). The multifaceted circulating endothelial cell in cancer: towards marker and target identification. Nat. Rev. Cancer *6*, 835–845.

Bussolati, B., Deambrosis, I., Russo, S., Deregibus, M.C., and Camussi, G. (2003). Altered angiogenesis and survival in human tumor-derived endothelial cells. FASEB J. *17*, 1159–1161.

Bussolati, B., Bruno, S., Grange, C., Buttiglieri, S., Deregibus, M.C., Cantino, D., and Camussi, G. (2005). Isolation of renal progenitor cells from adult human kidney. Am. J. Pathol. *166*, 545–555.

Chung, L.W. (2003). Prostate carcinoma bone-stroma interaction and its biologic and therapeutic implications. Cancer *97*, 772–778.

Collett, G.D., and Canfield, A.E. (2005). Angiogenesis and pericytes in the initiation of ectopic calcification. Circ. Res. *96*, 930–938.

Davidoff, A.M., Ng, C.Y., Brown, P., Leary, M.A., Spurbeck, W.W., Zhou, J., Horwitz, E., Vanin, E.F., and Nienhuis, A.W. (2001). Bone marrow-derived cells contribute to tumor neovasculature and, when modified to express an angiogenesis inhibitor, can restrict tumor growth in mice. Clin. Cancer Res. *7*, 2870–2879.

DeRuiter, M.C., Poelmann, R.E., VanMunsteren, J.C., Mironov, V., Markwald, R.R., and Gittenberger-de Groot, A.C. (1997). Embryonic endothelial cells transdifferentiate into mesenchymal cells expressing smooth muscle actins in vivo and in vitroCirc. Res. *80*, 444–451.

Doherty, M.J., Ashton, B.A., Walsh, S., Beresford, J.N., Grant, M.E., and Canfield, A.E. (1998). Vascular pericytes express osteogenic potential in vitro and in vivo. J. Bone Miner. Res. *13*, 828–838.

Duda, D.G., Cohen, K.S., Kozin, S.V., Perentes, J.Y., Fukumura, D., Scadden, D.T., and Jain, R.K. (2006). Evidence for incorporation of bone marrow-derived endothelial cells into perfused blood vessels in tumors. Blood *107*, 2774–2776.

Edlund, M., Sung, S.Y., and Chung, L.W. (2004). Modulation of prostate cancer growth in bone microenvironments. J. Cell. Biochem. *91*, 686–705.

Farrington-Rock, C., Crofts, N.J., Doherty, M.J., Ashton, B.A., Griffin-Jones, C., and Canfield, A.E. (2004). Chondrogenic and adipogenic potential of microvascular pericytes. Circulation *110*, 2226–2232.

Folkman, J. (2007). Angiogenesis: an organizing principle for drug discovery? Nat. Rev. Drug Discov. *6*, 273–286.

Gao, D., Nolan, D.J., Mellick, A.S., Bambino, K., McDonnell, K., and Mittal, V. (2008). Endothelial progenitor cells control the angiogenic switch in mouse lung metastasis. Science *319*, 195–198.

Greenberg, N.M., DeMayo, F., Finegold, M.J., Medina, D., Tilley, W.D., Aspinall, J.O., Cunha, G.R., Donjacour, A.A., Matusik, R.J., and Rosen, J.M. (1995). Prostate cancer in a transgenic mouse. Proc. Natl. Acad. Sci. USA *92*, 3439–3443.

Grover, A.C., Tangrea, M.A., Woodson, K.G., Wallis, B.S., Hanson, J.C., Chuaqui, R.F., Gillespie, J.W., Erickson, H.S., Bonner, R.F., Pohida, T.J., et al. (2006). Tumor-associated endothelial cells display GSTP1 and RARbeta2 promoter methylation in human prostate cancer. J. Transl. Med. *4*, 13.

Hagendoorn, J., Tong, R., Fukumura, D., Lin, Q., Lobo, J., Padera, T.P., Xu, L., Kucherlapati, R., and Jain, R.K. (2006). Onset of abnormal blood and lymphatic vessel function and interstitial hypertension in early stages of carcinogenesis. Cancer Res. *66*, 3360–3364.

Hegele, A., Wahl, H.G., Varga, Z., Sevinc, S., Koliva, L., Schrader, A.J., Hofmann, R., and Olbert, P. (2007). Biochemical markers of bone turnover in patients with localized and metastasized prostate cancer. BJU Int. *99*, 330–334.

Hendrix, M.J., Seftor, E.A., Meltzer, P.S., Gardner, L.M., Hess, A.R., Kirschmann, D.A., Schatteman, G.C., and Seftor, R.E. (2001). Expression and functional significance of VE-cadherin in aggressive human melanoma cells: role in vasculogenic mimicry. Proc. Natl. Acad. Sci. USA *98*, 8018–8023.

Hendrix, M.J., Seftor, E.A., Seftor, R.E., Kasemeier-Kulesa, J., Kulesa, P.M., and Postovit, L.M. (2007). Reprogramming metastatic tumour cells with embryonic microenvironments. Nat. Rev. Cancer *7*, 246–255.

Hida, K., Hida, Y., Amin, D.N., Flint, A.F., Panigrahy, D., Morton, C.C., and Klagsbrun, M. (2004). Tumor-associated endothelial cells with cytogenetic abnormalities. Cancer Res. *64*, 8249–8255.

Hu, M., Yao, J., Cai, L., Bachman, K.E., van den Brule, F., Velculescu, V., and Polyak, K. (2005). Distinct epigenetic changes in the stromal cells of breast cancers. Nat. Genet. *37*, 899–905.

Ingram, D.A., Mead, L.E., Tanaka, H., Meade, V., Fenoglio, A., Mortell, K., Pollok, K., Ferkowicz, M.J., Gilley, D., and Yoder, M.C. (2004). Identification of a novel hierarchy of endothelial progenitor cells using human peripheral and umbilical cord blood. Blood *104*, 2752–2760.

Ingram, D.A., Mead, L.E., Moore, D.B., Woodard, W., Fenoglio, A., and Yoder, M.C. (2005). Vessel wall-derived endothelial cells rapidly proliferate because they contain a complete hierarchy of endothelial progenitor cells. Blood *105*, 2783–2786.

Jiang, Y., Jahagirdar, B.N., Reinhardt, R.L., Schwartz, R.E., Keene, C.D., Ortiz-Gonzalez, X.R., Reyes, M., Lenvik, T., Lund, T., Blackstad, M., et al. (2002). Pluripotency of mesenchymal stem cells derived from adult marrow. Nature *418*, 41–49.

Johnson, R.C., Leopold, J.A., and Loscalzo, J. (2006). Vascular calcification: pathobiological mechanisms and clinical implications. Circ. Res. *99*, 1044–1059.

Kang, Y., Siegel, P.M., Shu, W., Drobnjak, M., Kakonen, S.M., Cordon-Cardo, C., Guise, T.A., and Massague, J. (2003). A multigenic program mediating breast cancer metastasis to bone. Cancer Cell *3*, 537–549.

Kitamura, T., Onishi, M., Kinoshita, S., Shibuya, A., Miyajima, A., and Nolan, G.P. (1995). Efficient screening of retroviral cDNA expression libraries. Proc. Natl. Acad. Sci. USA *92*, 9146–9150.

Koeneman, K.S., Yeung, F., and Chung, L.W. (1999). Osteomimetic properties of prostate cancer cells: a hypothesis supporting the predilection of prostate cancer metastasis and growth in the bone environment. Prostate *39*, 246–261.

Larrivee, B., Niessen, K., Pollet, I., Corbel, S.Y., Long, M., Rossi, F.M., Olive, P.L., and Karsan, A. (2005). Minimal contribution of marrow-derived endothelial precursors to tumor vasculature. J. Immunol. *175*, 2890–2899.

Lee, W.S., Jain, M.K., Arkonac, B.M., Zhang, D., Shaw, S.Y., Kashiki, S., Maemura, K., Lee, S.L., Hollenberg, N.K., Lee, M.E., and Haber, E. (1998). Thy-1, a novel marker for angiogenesis upregulated by inflammatory cytokines. Circ. Res. *82*, 845–851.

Lyden, D., Young, A.Z., Zagzag, D., Yan, W., Gerald, W., O'Reilly, R., Bader, B.L., Hynes, R.O., Zhuang, Y., Manova, K., and Benezra, R. (1999). Id1 and Id3 are required for neurogenesis, angiogenesis and vascularization of tumour xenografts. Nature *401*, 670–677.

Lyden, D., Hattori, K., Dias, S., Costa, C., Blaikie, P., Butros, L., Chadburn, A., Heissig, B., Marks, W., Witte, L., et al. (2001). Impaired recruitment of bone-marrow-derived endothelial and hematopoietic precursor cells blocks tumor angiogenesis and growth. Nat. Med. *7*, 1194–1201.

Machein, M.R., Renninger, S., de Lima-Hahn, E., and Plate, K.H. (2003). Minor contribution of bone marrow-derived endothelial progenitors to the vascularization of murine gliomas. Brain Pathol. *13*, 582–597.

McDonald, D.M., and Choyke, P.L. (2003). Imaging of angiogenesis: from microscope to clinic. Nat. Med. *9*, 713–725.

Nemoto, H., Rittling, S.R., Yoshitake, H., Furuya, K., Amagasa, T., Tsuji, K., Nifuji, A., Denhardt, D.T., and Noda, M. (2001). Osteopontin deficiency reduces experimental tumor cell metastasis to bone and soft tissues. J. Bone Miner. Res. *16*, 652–659.

Nolan, D.J., Ciarrocchi, A., Mellick, A.S., Jaggi, J.S., Bambino, K., Gupta, S., Heikamp, E., McDevitt, M.R., Scheinberg, D.A., Benezra, R., and Mittal, V. (2007). Bone marrow-derived endothelial progenitor cells are a major determinant of nascent tumor neovascularization. Genes Dev. *21*, 1546–1558.

O'Neill, T.J., 4th, Wamhoff, B.R., Owens, G.K., and Skalak, T.C. (2005). Mobilization of bone marrow-derived cells enhances the angiogenic response to hypoxia without transdifferentiation into endothelial cells. Circ. Res. *97*, 1027–1035.

Ozawa, M.G., Yao, V.J., Chanthery, Y.H., Troncoso, P., Uemura, A., Varner, A.S., Kasman, I.M., Pasqualini, R., Arap, W., and McDonald, D.M. (2005). Angiogenesis with pericyte abnormalities in a transgenic model of prostate carcinoma. Cancer *104*, 2104–2115.

Paruchuri, S., Yang, J.H., Aikawa, E., Melero-Martin, J.M., Khan, Z.A., Loukogeorgakis, S., Schoen, F.J., and Bischoff, J. (2006). Human pulmonary valve progenitor cells exhibit endothelial/mesenchymal plasticity in response to vascular endothelial growth factor-A and transforming growth factor-beta2. Circ. Res. *99*, 861–869.

Pittenger, M.F., Mackay, A.M., Beck, S.C., Jaiswal, R.K., Douglas, R., Mosca, J.D., Moorman, M.A., Simonetti, D.W., Craig, S., and Marshak, D.R. (1999). Multilineage potential of adult human mesenchymal stem cells. Science *284*, 143–147.

Prockop, D.J. (1997). Marrow stromal cells as stem cells for nonhematopoietic tissues. Science *276*, 71–74.

Rajantie, I., Ilmonen, M., Alminaite, A., Ozerdem, U., Alitalo, K., and Salven, P. (2004). Adult bone marrow-derived cells recruited during angiogenesis comprise precursors for periendothelial vascular mural cells. Blood *104*, 2084–2086.

Reyes, M., Lund, T., Lenvik, T., Aguiar, D., Koodie, L., and Verfaillie, C.M. (2001). Purification and ex vivo expansion of postnatal human marrow mesodermal progenitor cells. Blood *98*, 2615–2625.

Santarelli, J.G., Udani, V., Yung, Y.C., Cheshier, S., Wagers, A., Brekken, R.A., Weissman, I., and Tse, V. (2006). Incorporation of bone marrow-derived Flk-1-expressing CD34+ cells in the endothelium of tumor vessels in the mouse brain. Neurosurgery *59*, 374–382.

Seaman, S., Stevens, J., Yang, M.Y., Logsdon, D., Graff-Cherry, C., and St Croix, B. (2007). Genes that distinguish physiological and pathological angiogenesis. Cancer Cell *11*, 539–554.

Spangrude, G.J., Heimfeld, S., and Weissman, I.L. (1988). Purification and characterization of mouse hematopoietic stem cells. Science *241*, 58–62.

St Croix, B., Rago, C., Velculescu, V., Traverso, G., Romans, K.E., Montgomery, E., Lal, A., Riggins, G.J., Lengauer, C., Vogelstein, B., and Kinzler, K.W. (2000). Genes expressed in human tumor endothelium. Science *289*, 1197–1202.

Streubel, B., Chott, A., Huber, D., Exner, M., Jager, U., Wagner, O., and Schwarzinger, I. (2004). Lymphoma-specific genetic aberrations in microvascular endothelial cells in B-cell lymphomas. N. Engl. J. Med. *351*, 250–259.

Takahashi, T., Kalka, C., Masuda, H., Chen, D., Silver, M., Kearney, M., Magner, M., Isner, J.M., and Asahara, T. (1999). Ischemia- and cytokine-induced mobilization of bone marrow-derived endothelial progenitor cells for neovascularization. Nat. Med. *5*, 434–438.

Tintut, Y., Alfonso, Z., Saini, T., Radcliff, K., Watson, K., Bostrom, K., and Demer, L.L. (2003). Multilineage potential of cells from the artery wall. Circulation *108*, 2505–2510.

Topczewska, J.M., Postovit, L.M., Margaryan, N.V., Sam, A., Hess, A.R., Wheaton, W.W., Nickoloff, B.J., Topczewski, J., and Hendrix, M.J. (2006). Embryonic and tumorigenic pathways converge via Nodal signaling: role in melanoma aggressiveness. Nat. Med. *12*, 925–932.

Udagawa, T., Puder, M., Wood, M., Schaefer, B.C., and D'Amato, R.J. (2006). Analysis of tumor-associated stromal cells using SCID GFP transgenic mice: contribution of local and bone marrow-derived host cells. FASEB J. *20*, 95–102.

van de Rijn, M., Heimfeld, S., Spangrude, G.J., and Weissman, I.L. (1989). Mouse hematopoietic stem-cell antigen Sca-1 is a member of the Ly-6 antigen family. Proc. Natl. Acad. Sci. USA *86*, 4634–4638.

Wai, P.Y., and Kuo, P.C. (2008). Osteopontin: regulation in tumor metastasis. Cancer Metastasis Rev. *27*, 103–118.

Wang, H., Riha, G.M., Yan, S., Li, M., Chai, H., Yang, H., Yao, Q., and Chen, C. (2005). Shear stress induces endothelial differentiation from a murine embryonic mesenchymal progenitor cell line. Arterioscler. Thromb. Vasc. Biol. *25*, 1817–1823.

Wang, H., McKnight, N.C., Zhang, T., Lu, M.L., Balk, S.P., and Yuan, X. (2007). SOX9 is expressed in normal prostate basal cells and regulates androgen receptor expression in prostate cancer cells. Cancer Res. *67*, 528–536.

Watson, K.E., Bostrom, K., Ravindranath, R., Lam, T., Norton, B., and Demer, L.L. (1994). TGF-beta 1 and 25-hydroxycholesterol stimulate osteoblast-like vascular cells to calcify. J. Clin. Invest. *93*, 2106–2113.

Yamashita, J., Itoh, H., Hirashima, M., Ogawa, M., Nishikawa, S., Yurugi, T., Naito, M., Nakao, K., and Nishikawa, S. (2000). Flk1-positive cells derived from embryonic stem cells serve as vascular progenitors. Nature *408*, 92–96.

Yung, Y.C., Cheshier, S., Santarelli, J.G., Huang, Z., Wagers, A., Weissman, I., and Tse, V. (2004). Incorporation of naive bone marrow derived cells into the vascular architecture of brain tumor. Microcirculation *11*, 699–708.

Cancer Cell, Volume *14*

Supplemental Data

Article

Calcification of Multipotent

Prostate Tumor Endothelium

Andrew C. Dudley, Zia A. Khan, Shou-Ching Shih, Soo-Young Kang, Bernadette M.M. Zwaans, Joyce Bischoff, and Michael Klagsbrun

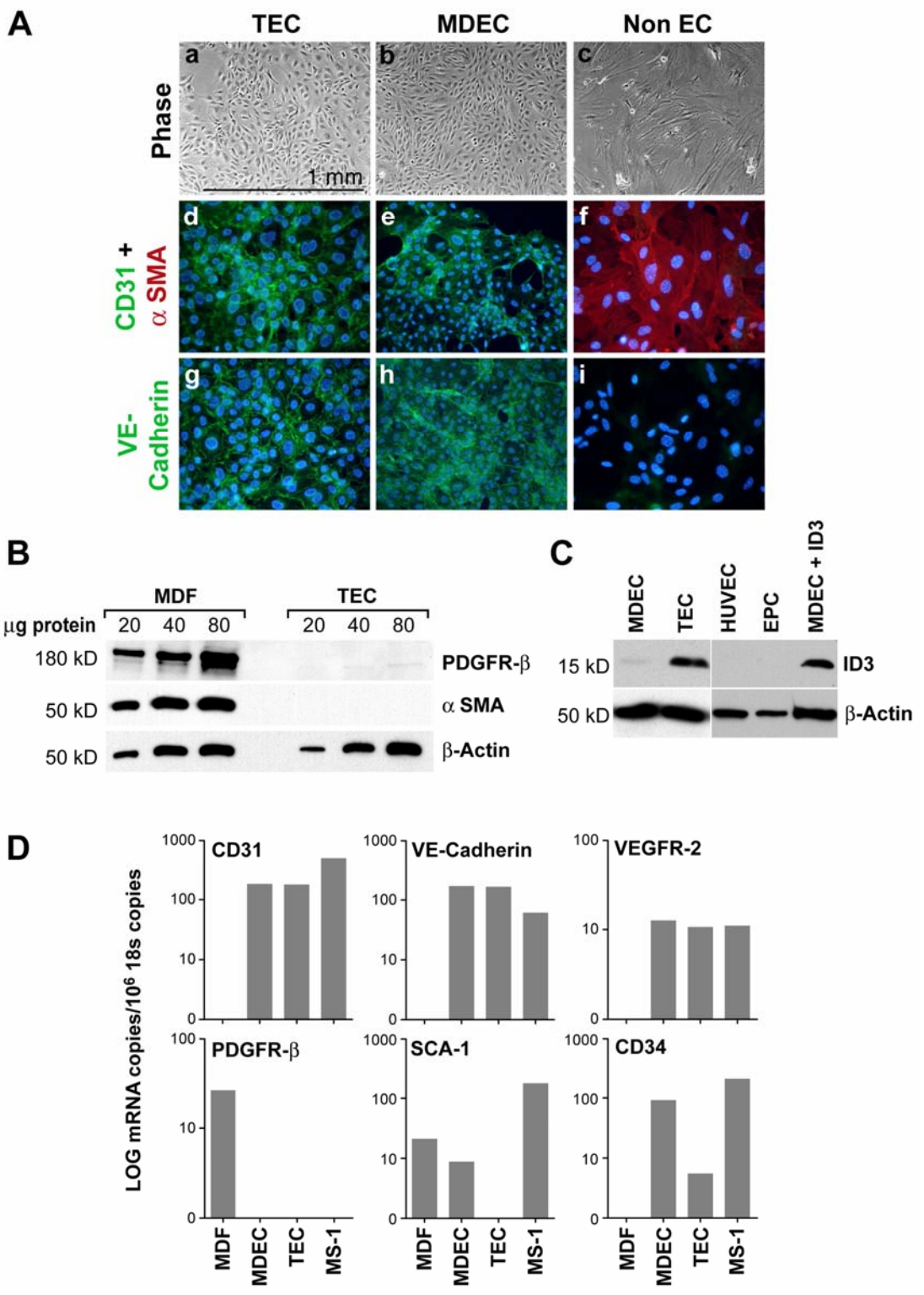
A
TEC
MDEC
Non EC
Phase
1 mm
CD31 + α SMA
VE-Cadherin
B
MDF
TEC
µg protein
20
40
80
180 kD
PDGFR-β
α SMA
50 kD
β-Actin
C
MDEC
TEC
HUVEC
EPC
MDEC + ID3
15 kD
ID3
50 kD
β-Actin
D
LOG mRNA copies/10^6 18s copies
CD31
VE-Cadherin
VEGFR-2
PDGFR-β
SCA-1
CD34
MDF
MDEC
TEC
MS-1

Figure S1.

Figure S1. Additional TEC Characterization

(A) Phase microscopy images of TECs (a) MDECs (b) and mesenchymal-like, non-ECs (c). By immunofluorescence, the isolated ECs uniformly expressed CD31 and VE-cadherin, but not α SMA (d-i).

(B) Western blot of pericyte/mesenchymal markers in TECs and mouse dermal fibroblasts (MDF).

(C) Western blot for ID3 in TECs versus MDECs. MDECs transiently transfected with an ID3 expression construct were included as a positive control.

(D) By real-time PCR, MDECs and TECs expressed mRNAs for endothelial-specific CD31, VE-cadherin, and VEGFR-2, but not the mural/mesenchymal marker PDGFR-β. TECs are low to absent for SCA-1 and CD34. The mouse MS-1 endothelial cell line served as a positive control.

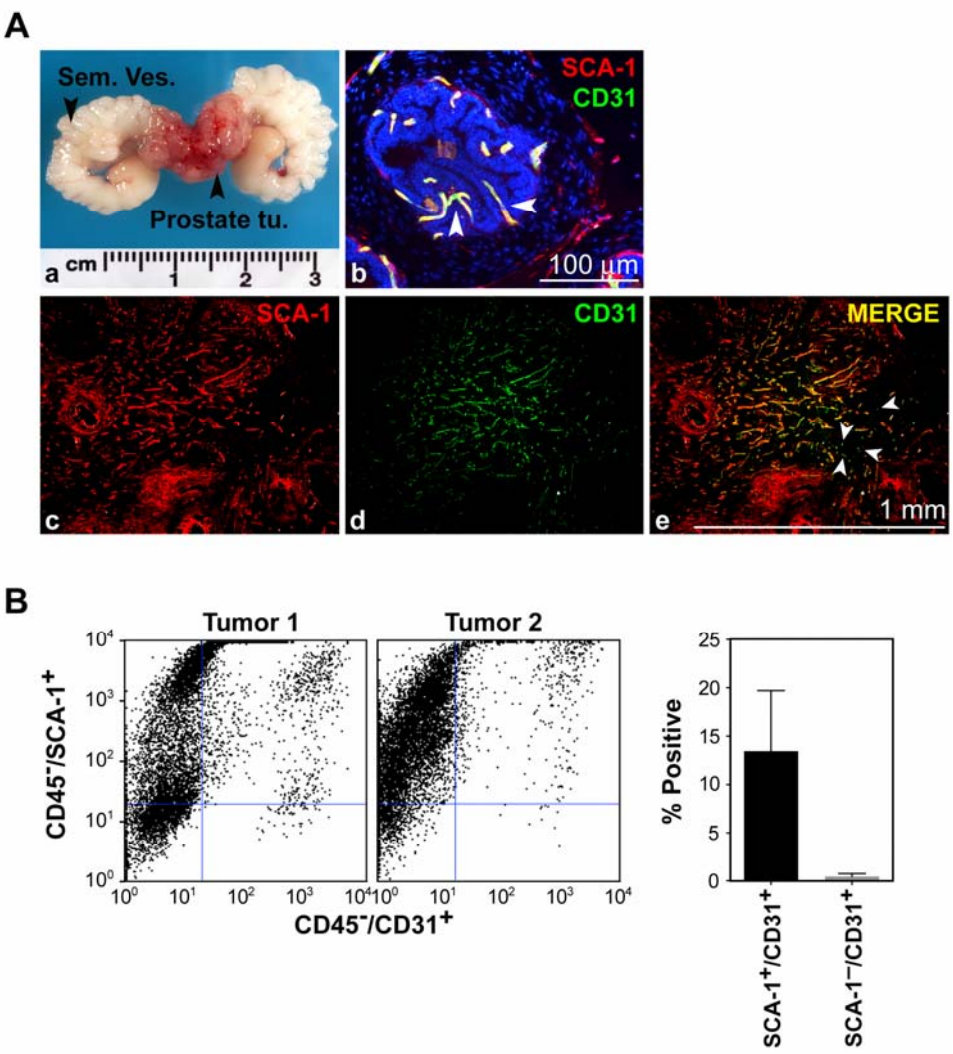

Figure S2. SCA-1$^-$/CD31$^+$ TECs Are Rare in TRAMP Prostate Tumors

(A) Genitourinary tract from a 30 week-old TRAMP mouse (a). A 6 µm section of the dorsolateral lobe showing that the majority of CD31$^+$ tumor blood vessels were also SCA-1$^+$ (yellow merge). The arrows point to two blood vessels co-expressing both markers (b). Lower magnification of a TRAMP prostate tumor showing extensive SCA-1$^+$ staining in the tumor blood vessels, fibroblastic-like stromal cells, and tumor epithelial ductules (c). The same field is shown in (d) and merged with the CD31 signal in (e). Only occasional CD31$^+$/SCA-1$^-$ cells can be observed (green cells, white arrowheads).

(B) Flow cytometry of two TRAMP prostate tumors. CD45$^+$ hematopoietic progenitors were excluded by out-gating. The percentage of single and double positive cells were plotted at right. Error bars are +/- SEM.

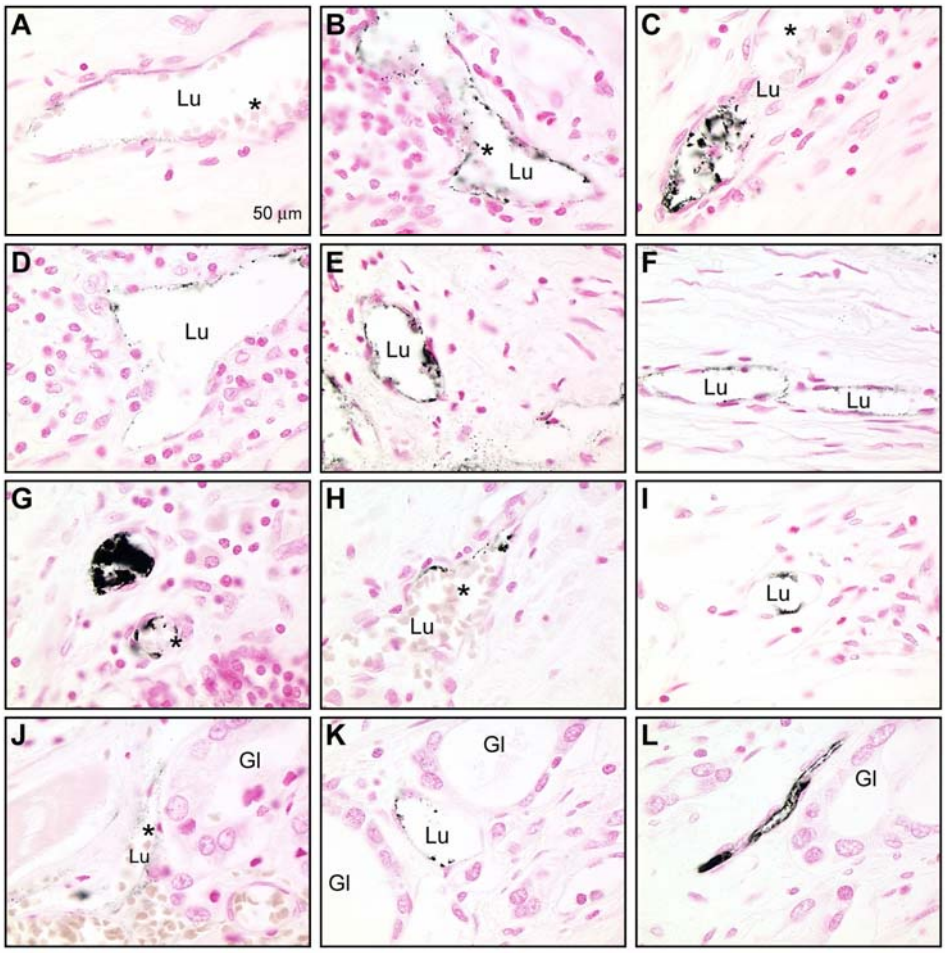

Figure S3. von Kossa Staining in Human Prostate Tumor Blood Vessels

Additional images of tumor blood vessels stained with von Kossa. An asterisk (*) marks erythrocytes where visible. Lu = Lumen and Gl = gland. The nuclei were counterstained with nuclear fast red.

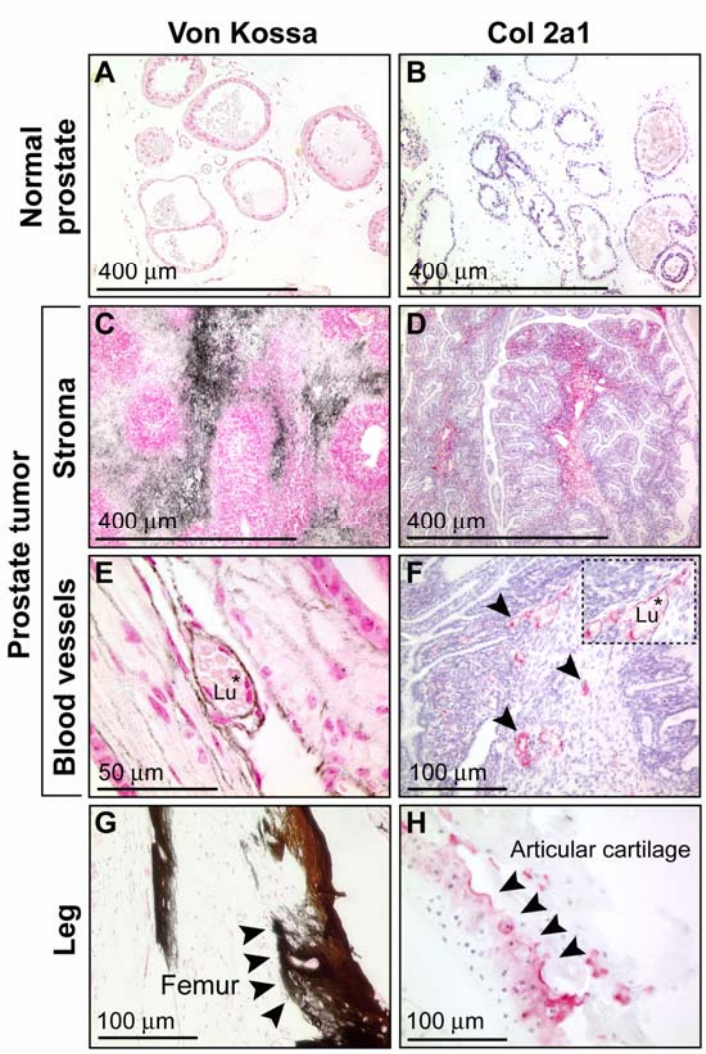

Figure S4. von Kossa and col2a1 Staining in TRAMP Prostate Tumors

Normal prostate stained with von Kossa (A) and col2a1 antibodies (B). Both von Kossa and col2a1 were detected in the tumor stroma (C and D) and tumor blood vessels (E and F). For all von Kossa staining, nuclei were counterstained with fast red. For all col2a1 staining, nuclei were lightly counterstained with hematoxylin. The boxed region in 'F' is a higher magnification of a tumor blood vessel. Lu = lumen and the asterisk (*) marks visible erythrocytes. The arrow heads in 'F' point to additional blood vessels. col2a1 was detected with an alkaline phosphatase-conjugated secondary antibody (red). Mouse leg was included as a positive control for von Kossa (G) and col2a1 (H).

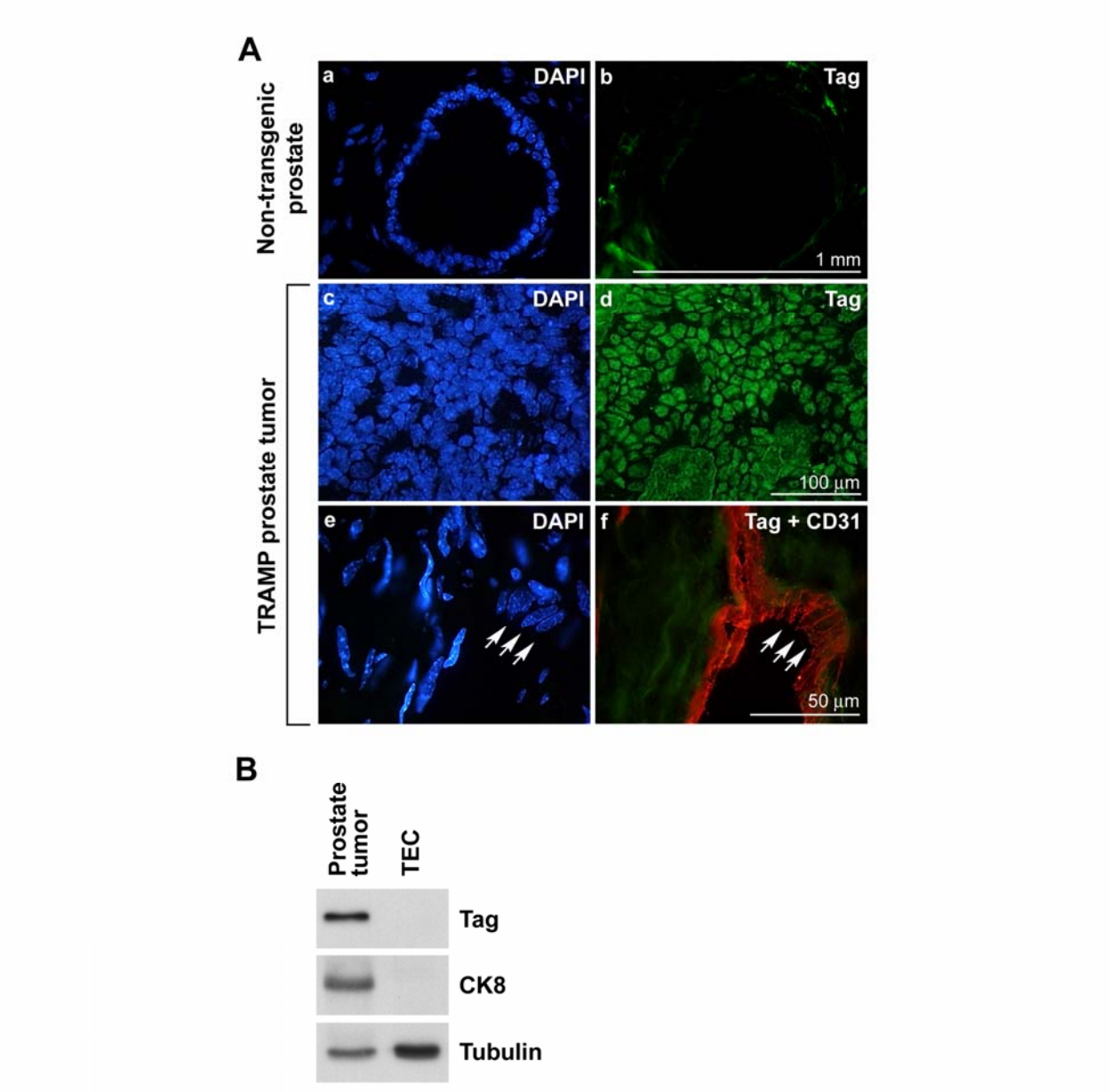

Figure S5. TECs Do Not Express T Antigen In Vivo or In Vitro

(A) In each field, the same dorsal-lateral lobe is shown stained with T antigen (Tag) antibodies or counterstained with DAPI. Prostates from non-transgenic mice were negative for Tag. Only diffuse background staining was evident, probably due to non-specific cross-reactivity of the mouse monoclonal Tag antibodies with mouse tissue (a-b). The nuclei of luminal epithelial cells from a TRAMP prostate tumor stained strongly for Tag (c-d). In contrast, tumor-associated endothelial cells in TRAMP prostate tumors were negative for Tag. The arrows point to three endothelial nuclei which are CD31 positive but Tag negative (e-f).

(B) Western blotting of tumors or isolated TECs (passage 10) confirmed the absence of both epithelial cytokeratin (CK8) and Tag expression.